Program Digest, 2019 IEEE International Ultrasonics Symposium (IUS)
Glasgow, Scotland, October 6-9, 2019

Pressure Difference Estimation in Carotid Bulbs using Vector Flow Imaging - A Phantom Study

Tin-Quoc Nguyen[1,2], Marie Sand Traberg[3], Jacob Bjerring Olesen[4], Ramin Moshavegh[4], Peter Hasse Møller-Sørensen[5], Lars Lönn[1,2], Jørgen Arendt Jensen[3], Michael Bachmann Nielsen[1,2], and Kristoffer Lindskov Hansen[1,2]

[1] Department of Diagnostic Radiology, Rigshospitalet, Copenhagen, Denmark
[2] Department of Clinical Medicine, University of Copenhagen, Copenhagen, Denmark
[3] Center for Fast Ultrasound Imaging, Department of Health Technology, Technical University of Denmark, Kgs. Lyngby, Denmark
[4] BK Medical Aps, Herlev, Denmark
[5] Department of Thoracic Anaesthesiology, Rigshospitalet, Copenhagen, Denmark

***Abstract*—Hypertension is a common health problem and may be caused by dysfunction of the stretch sensitive baroreceptors in the carotid bulb. Velocity changes and vortices are present in the carotid bulb, and a better evaluation of the local flow and pressures may be important to further understand hypertension. The intravascular pressure catheter is a common tool in the clinic and is currently considered to be the reference standard for intravascular pressure measurement, but the method is invasive, ionizing, and has been reported to be inaccurate. Vector flow imaging (VFI) is an angle independent, noninvasive, and nonionizing ultrasound method that can estimate pressure differences. In this study, pressure differences between the common carotid artery and the carotid bulb obtained with VFI were compared with catheter measurements in three carotid bifurcation phantoms. A fluid-structure interaction (FSI) simulation model was used as reference. Additionally, 10 repeated VFI and catheter measurements were performed in one phantom for a precision assessment. The mean absolute pressure difference between the catheter and FSI method in the three phantoms was 140.5 Pa, and 10 repeated catheter tests measured a mean pressure decrease with a large variation (mean: -133.3 Pa, SD: 786%). VFI estimated pressure increases in all phantoms with a mean standard deviation of 11.6%, and the mean absolute pressure difference compared with FSI was 16.7 Pa. Ten repeated VFI estimations found a mean pressure increase with low variation (mean: 40.1 Pa, SD: 10.9%). VFI precisely estimated small pressure differences in a carotid bifurcation phantom setup, whereas the fluid-filled pressure catheter measurements were imprecise.**

***Index Terms*—Pressure difference estimation, vector flow imaging, fluid-filled pressure catheter, fluid-structure interaction simulation, phantom study, carotid bifurcation**

I. Introduction

Blood pressure changes are detected by stretch sensitive baroreceptors in the carotid bulb. The baroreceptors relay the information onward to the brain stem, where control centers regulate heart rate and peripheral vascular resistance to maintain homeostasis [1]. The carotid bulb is an enlargement of the proximal part of the internal carotid artery. In the bulb, blood flow tends to decelerate [2], [3], forming a slow moving vortex, which increases the blood pressure locally according to the principle of conservation of energy [4]. The carotid bulb and vortex have been hypothesized to serve as an amplifier for the baroreceptors that indirectly manage the blood pressure [5]. Therefore, dysfunction of the baroreceptors or carotid vortex may be connected with hypertension [6], and pressure difference evaluation in the carotid bulb may be of importance in the understanding and treatment of this medical condition.

The intravascular fluid-filled pressure catheter is currently considered the clinical reference standard for measuring intravascular pressure differences [7], but it is an invasive and time-consuming method that is associated with complications [8], [9] and requires ionizing radiation for guidance. Accordingly, noninvasive alternatives have been developed, and pressure differences can now easily be derived from velocity estimations obtained with spectral Doppler ultrasound by applying the simplified Bernoulli equation [4]. However, the accuracy of this approach is limited by its negligence of energy losses and delicacy to incorrect velocity estimation due to erroneous beam-to-flow angle adjustment [10], [11]. Vector flow imaging (VFI) is an angle independent flow estimation method for ultrasound that obtains 2D velocity vectors [12]. The method allows pressure differences to be calculated along a streamline by applying the unsteady Bernoulli equation to the 2D vector accelerations [13].

We undertook a study with the aim of evaluating a VFI approach for estimating small intravascular pressure differences. Three carotid phantoms were catheterized and scanned with VFI in an experimental controlled setup. VFI-derived pressure differences were hypothesized to be more precise than catheter measurements. The pressure differences were compared with a fluid-structure interaction (FSI) simulation model for reference.

II. Methods

A. Experimental Setup

Three carotid bifurcation phantoms were fabricated based on magnetic resonance imaging data from three healthy volunteers. The manufacturing process has been described in previous papers [13], [14]. A flow system (CompuFlow 1000, Shelley Medical Imaging Technologies, Toronto, Canada) was used to generate a time-varying flow to the blood-mimicking fluid (BMF-US, Shelley Medical Imaging Technologies, Toronto, Canada). The dynamic flow had a waveform comparable to the *in vivo* carotid flow with a peak volume flow of 25 mL/s in all measurements.

B. Catheter Measurements

Catheterization was performed through an arterial sheath using a 4 French fluid-filled catheter connected to a pressure monitor (IntelliVue X2, Philips Medizin Systeme, Boeblingen, Germany). The tip of the catheter was navigated to the common carotid artery under ultrasound guidance, where the pressure monitor was calibrated and a peak pressure was recorded after the readings had stabilized. Subsequently, the catheter was navigated to the carotid bulb, where a second peak pressure was measured without recalibration. In one phantom, 10 calibrations and peak pressure differences were measured for a precision assessment.

C. VFI Data Acquisition

A 5.5 MHz linear transducer (BK Medical Aps, Herlev, Denmark) was positioned to fit the carotid bifurcation inside the color box for VFI, see Fig. 1. Data were obtained at a rate of 30 frames per second for 13 seconds and stored on the scanner (bk5000, BK Medical Aps, Herlev, Denmark). The pulse repetition frequency was set to the lowest setting that did not cause any aliasing on the scanner display. Ten consecutive acquisitions were obtained for one phantom for a precision assessment. Data were processed and analyzed using an in-house built program [15] in MATLAB (MathWorks, Natick, MA, USA). A streamline was drawn in free hand between the two catheter positions, and the pressure difference was derived by applying the unsteady Bernoulli equation [13]:

$$\Delta P(t) = -\rho \left[\frac{v_{s,l_2}^2 - v_{s,l_1}^2}{2} + \int_{l_1}^{l_2} \frac{\partial v_s}{\partial t} ds \right], \qquad (1)$$

where ΔP is the summed pressure difference along the streamline between position l_1 and l_2, rho is the density of the fluid, and v_s is the scalar product of $\vec{v}(\vec{r},t)$. The out-of-plane component was assumed to be zero as VFI only acquires vectors in two dimensions. Drawing a streamline inside the program produced a graph showing the highest systolic pressure difference along the streamline with a standard deviation (SD) across all systoles.

D. Fluid-Structure Interaction Models

The flow in the FSI model of the carotid artery is described by the Navier-Stokes equation assuming that the fluid is incompressible and Newtonian,

$$\rho \left(\frac{\partial \vec{v}}{\partial t} + \vec{v} \cdot \nabla \vec{v} \right) = -\nabla p + \eta \nabla^2 \vec{v} + \rho \vec{g} \quad , \qquad (2)$$

where $\rho = 1,030$ kg/m^3 is the density of the blood-mimicking fluid, $\vec{v}$ is the computed velocity field, which is a function

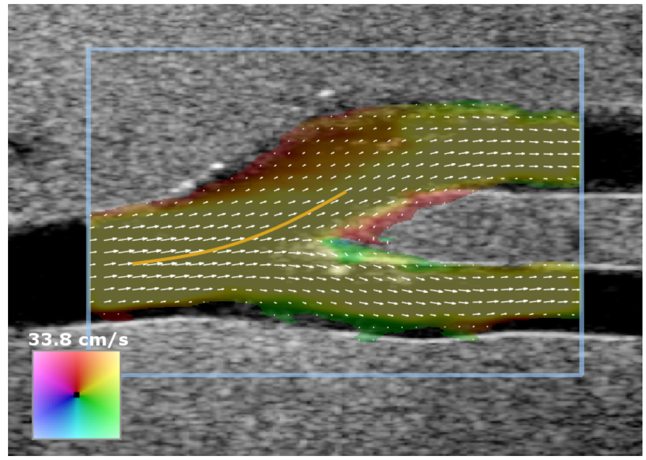

Fig. 1. VFI image of peak systole in a carotid bifurcation phantom. Flow direction and magnitude are indicated by the color wheel. A pressure difference is estimated along the orange streamline. The illustrated VFI box was 2 cm in height and 3 cm in width and was adjusted manually for each phantom.

of all three spatial dimensions (x, y, z) and time (t), p is pressure, $\eta = 4.1$ mPa·s is the fluid viscosity, and $\vec{g}$ is gravity. The solid surrounding the fluid domain consisted of polyvinyl alcohol (PVA) cryogel, a tissue-mimicking polymer material that allows the elasticity to be controlled during fabrication. The fabrication process was the same as described by Olesen et al. [13]. The PVA was assumed to have a Young's modulus of 106.1 kPa [16] and a Poisson's ratio of 0.49. The polymer was modelled as a hyper-elastic material to allow finite strains, as deformations of 7-10% have been observed in in-house experiments. This corresponds to *in vivo* data, where dilation of 10-15% has been reported [17]. A Neo-Hookean type strain-energy function was used to simulate the solid response to the fluid dynamics in the fluid domain,

$$\psi = \frac{\mu}{2} (I_1 - 3) \quad , \qquad (3)$$

where ψ is the strain-energy, μ is the shear modulus, and I_1 is the first principal invariant of the right Cauchy-Green tensor. The shear modulus is derived from Young's modulus, E, and Poisson's ratio, ν,

$$\mu = \frac{E}{2(1+\nu)} \quad . \qquad (4)$$

To allow the fluid-structure interaction, i.e. motion of the boundary between the fluid and the solid, the two constitutive relations were formulated relative to the same coordinate system. The interacting boundary between the fluid and the solid was handled in the finite element method by an Arbitrary Lagrangian-Eulerian (ALE) implementation, where the physical equations for the fluid and the solid were reformulated with respect to the mesh coordinates. All FSI model simulations were conducted in COMSOL Multiphysics v5.4 (COMSOL AB, Stockholm, Sweden).

A mesh convergence study was carried out for one of the three individual FSI models. The meshing of the fluid and solid domain was performed using the build-in teslation methods in COMSOL Multiphysics optimised to handle FSI. A mesh with $5.5 \cdot 10^5$ degrees-of-freedom (number of mesh nodes times number of values calculated in each node) gave a precision of ± 2 %.

The inlet boundary conditions of the FSI models were obtained from the measured mean spatial velocity profile in each phantom. The principles of Womersley and Evans were used to reconstruct a smooth continuous velocity profile as a function of time and space [18], [19]. The outlet conditions were pressures adapted to deliver the measured volume flow in each branch.

III. Results

The single pressure difference measurements for the three carotid phantoms and the 10 repeated measurements for one carotid phantom are listed in Table I and II.

TABLE I
SINGLE PRESSURE DIFFERENCE MEASUREMENTS IN THREE PHANTOMS

	Catheter [Pa]	**VFI [Pa] *(SD)***	**FSI [Pa]**
Carotid 1	0	45.2 *(14%)*	37.3
Carotid 2	266.7	40.3 *(12%)*	33.5
Carotid 3	0	115.2 *(8%)*	150.6

TABLE II
REPEATED PRESSURE DIFFERENCE MEASUREMENTS IN ONE PHANTOM

	Catheter [Pa]	**VFI [Pa] *(SD)***
1	0	40.3 *(12%)*
2	2000	43.5 *(8%)*
3	0	39.5 *(8%)*
4	0	38.3 *(14%)*
5	0	36.7 *(9%)*
6	133	38.9 *(6%)*
7	0	39.1 *(19%)*
8	0	41.3 *(8%)*
9	-1600	42.0 *(10%)*
10	-1867	41.2 *(9%)*

The catheter measured a pressure increase in one phantom and no difference in two. VFI and FSI estimated pressure increases in all phantoms, and VFI had a mean SD of 11.6% between pulse cycles. VFI overestimated FSI in two phantoms and underestimated in one. Ten repeated catheter measurements found a mean pressure drop with a large variation (mean: -133.3 Pa, SD: 786%) compared with VFI (mean: 40.1 Pa, SD: 10.9%). The mean absolute pressure difference was 140.5 Pa between catheter measurements and FSI, and 16.7 Pa between VFI and FSI. A comparison between VFI and FSI is illustrated in Fig. 2, and the 10 repeated VFI measurements are plotted in Fig. 3.

IV. Discussion

The VFI method agreed with the FSI simulations and found a pressure increase from the common carotid artery to the carotid bulb in all phantoms, whereas the pressure catheter only found an increase in one. Additionally, the VFI method

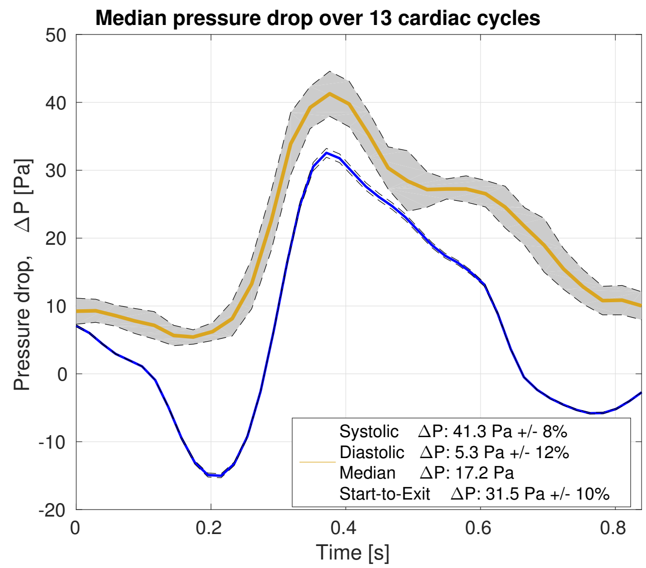

Fig. 2. Comparison of VFI- and FSI-derived pressure difference in the bifurcation of *Carotid 2*. The orange line is the VFI-derived pressure difference during a cycle and the blue line is from the FSI model.

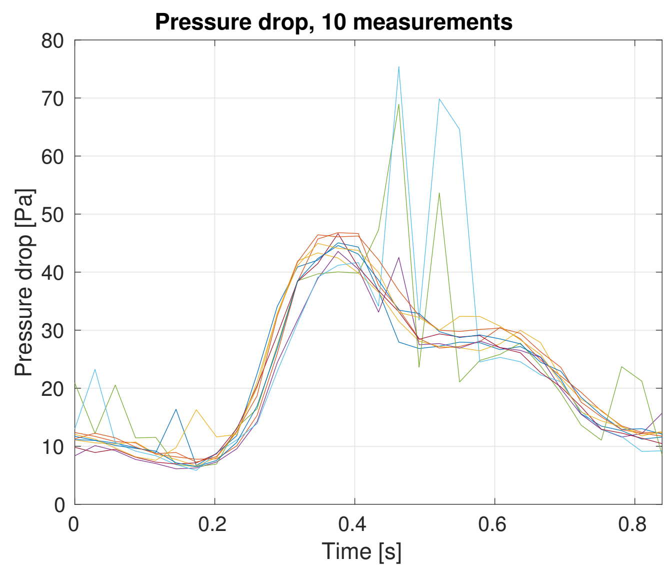

Fig. 3. Ten consecutive VFI pressure difference estimations in *Carotid 2*.

followed the same trend as FSI and identified the phantoms with the highest and lowest pressure difference.

Many conventional ultrasound scanners derive pressure differences by applying the simplified Bernoulli equation [11], which only requires a single peak velocity estimate [4]. However, the equation assumes that the velocity difference between two positions is sufficiently great that one can be neglected, which is not true in nonstenotic carotid bifurcations [2], [3] and will result in severe overestimation. The VFI method uses the unsteady Bernoulli equation (1) that calculates a pressure difference between each velocity vector before summing, allowing it to be used for small velocity changes.

VFI managed to estimate pressure differences that were lower than our pressure monitor could differentiate. The pressure monitor had limited sensitivity and could only measure pressures in the increment of ± 1 mmHg (≈ 133.3 Pa); more than three times higher than VFI measured during the repeated scans. This limitation can partially explain the high SD observed for the catheter measurements. Another factor was three outliers among the catheter measurements that we were unable to explain. Furthermore, catheterization requires introduction of a foreign object into the bloodstream, thus altering the blood flow and pressures from the initial conditions [20].

A discrepancy of $\pm$ 5-10 mmHg between catheter and noninvasive methods has previously been considered as clinically acceptable [21], [22]. However, the invasive practice of the fluid-filled catheter, the inaccuracy [20], and the high imprecision observed in our study challenges the catheter as an ideal reference method. Precise evaluation of vortices and pressure differences in the carotid bulb may be important for understanding hypertension [5], [6], and correct diagnosis can ultimately result in alleviation of symptoms or even treatment of the disease.

VFI is an angle independent and noninvasive ultrasound method for flow evaluation. The method offers an opportunity for real-time visualization of flow and excellent precision for pressure difference estimation, which can be used to deepen our understanding of physiology and characterize the complex hemodynamics surrounding e.g. the baroreceptors, venous valves, and cardiac valves.

This study had several limitations. Firstly, VFI obtains velocity vectors in 2D and assumes vectors in the third spatial dimension to be zero. The vortex is a known phenomenon in the carotid bulb [5], and the out-of-plane component may be significant. Secondly, VFI acquisitions were obtained with a hand-held transducer, and operator-induced movements may have resulted in a larger SD. Lastly, streamlines were drawn in free-hand, and the 2D streamlines drawn for VFI may not have been replicated accurately enough for the FSI analyses.

V. Conclusion

VFI was used to estimate small pressure differences in carotid bifurcation phantoms and had higher precision compared with a fluid-filled pressure catheter. A pressure increase was found in all phantoms with both VFI and FSI, and both methods followed the same trend for pressure differences between the phantoms. VFI-derived pressure differences displayed similar variation for single pressure measurements and repeated measurements, indicating that the method remained consistent across different phantom models. VFI offers an angle independent, noninvasive, and more precise method for intravascular pressure difference estimation that can increase diagnostic certainty, ultimately aiding the clinician in determining the most appropriate option of treatment.

References

[1] M. Di Rienzo, G. Parati, A. Radaelli, and P. Castiglioni, “Baroreflex contribution to blood pressure and heart rate oscillations: time scales, time-variant characteristics and nonlinearities,” *Philos Trans A Math Phys Eng Sci*, vol. 367, no. 1892, pp. 1301–1318, 2009.

[2] W. M. Blackshear *et al.*, “Carotid artery velocity patterns in normal and stenotic vessels.” *Stroke*, vol. 11, no. 1, pp. 67–71, 1980.

[3] J. Kochanowicz *et al.*, “Normal reference values of ratios of blood flow velocities in internal carotid artery to those in common carotid artery using doppler sonography,” *J Clin Ultrasound*, vol. 37, no. 4, pp. 208–211, 2009.

[4] A. P. Yoganathan, E. G. Cape, H.-W. Sung, F. P. Williams, and A. Jimoh, “Review of hydrodynamic principles for the cardiologist: Applications to the study of blood flow and jets by imaging techniques,” *J. Am. Coll. Cardiol.*, vol. 12, no. 5, pp. 1344–1353, 1988.

[5] K. L. Hansen, *In-vivo studies of new vector velocity and adaptive spectral estimators in medical ultrasound*. Dan Med Bull., 2010, vol. 57(5), pp. 1-23.

[6] P. Kougias, S. M. Weakley, Q. Yao, P. H. Lin, and C. Chen, “Arterial baroreceptors in the management of systemic hypertension,” *Med Sci Monitor*, vol. 16, no. 1, pp. RA1–RA8, 2010.

[7] J. Bock *et al.*, “In vivo noninvasive 4D pressure difference mapping in the human aorta: phantom comparison and application in healthy volunteers and patients,” *Magn. Reson. Med.*, vol. 66, no. 4, pp. 1079–1088, 2011.

[8] L. A. Mermel, “Prevention of intravascular catheter-related infections,” *Ann Intern Med*, vol. 132, no. 5, p. 391, 2000.

[9] H. Omran *et al.*, “Silent and apparent cerebral embolism after retrograde catheterisation of the aortic valve in valvular stenosis: a prospective, randomised study,” *The Lancet*, vol. 361, no. 9365, pp. 1241–1246, 2003.

[10] L. Hatle, B. A. Angelsen, and A. Tromsdal, “Non-invasive assessment of aortic stenosis by doppler ultrasound,” *Br Heart J*, vol. 43, no. 3, pp. 284–292, 1980.

[11] F. Donati *et al.*, “Beyond Bernoulli - Improving the accuracy and precision of noninvasive estimation of peak pressure drops,” *Circ Cardiovasc Imaging*, pp. 1–9, 2017.

[12] J. A. Jensen and P. Munk, “A new method for estimation of velocity vectors,” *IEEE Trans. Ultrason., Ferroelec., Freq. Contr.*, vol. 45, no. 3, pp. 837–851, 1998.

[13] J. B. Olesen *et al.*, “Non-invasive estimation of pressure changes using 2-D vector velocity ultrasound: An experimental study with in-vivo examples,” *IEEE Trans. Ultrason., Ferroelec., Freq. Contr.*, vol. 65, no. 5, pp. 709–719, 2018.

[14] S. S. M. Lai, B. Y. S. Yiu, A. K. K. Poon, and A. C. H. Yu, “Design of anthropomorphic flow phantoms based on rapid prototyping of compliant vessel geometries,” *Ultrasound Med. Biol.*, vol. 39, no. 9, pp. 1654–1664, 2013.

[15] R. Moshavegh *et al.*, “Hybrid segmentation of vessels and automated flow measures in in-vivo ultrasound imaging,” in *Proc. IEEE Ultrason. Symp.*, Sep 2016, pp. 1–4.

[16] R. K. W. Chee, A. Sampaleanu, D. Rishi, and R. J. Zemp, “Top orthogonal to bottom electrode (TOBE) 2-D CMUT arrays for 3-D photoacoustic imaging,” *IEEE Trans. Ultrason., Ferroelec., Freq. Contr.*, vol. 61, no. 8, pp. 1393–1395, 2014.

[17] J. O. Arndt, J. Klauske, and F. Mersch, “The diameter of the intact carotid artery in man and its change with pulse pressure,” *Pflugers Archiv*, vol. 301, pp. 230–240, 1968.

[18] J. A. Jensen, *Estimation of Blood Velocities Using Ultrasound: A Signal Processing Approach*. New York: Cambridge University Press, 1996.

[19] J. Jensen *et al.*, “Accuracy and precision of a plane wave vector flow imaging method in the healthy carotid artery,” *Ultrasound Med. Biol.*, vol. 44, no. 8, pp. 1727–1741, 2018.

[20] A. de Vecchi *et al.*, “Catheter-induced errors in pressure measurements in vessels: An in-vitro and numerical study,” *IEEE Trans. Biomed. Eng.*, vol. 61, no. 6, pp. 1844–1850, 2014.

[21] M. R. Fisher *et al.*, “Accuracy of doppler echocardiography in the hemodynamic assessment of pulmonary hypertension,” *Am J Resp Crit Care*, vol. 179, no. 7, pp. 615–621, 2009.

[22] R. D. Laver, U. F. Wiersema, and A. D. Bersten, “Echocardiographic estimation of mean pulmonary artery pressure in critically ill patients,” *Crit Ultrasound J*, vol. 6, no. 1, pp. 1–7, 2014.